Importance of Packing Coefficients of Host Cavities in the Isomerization of Open Host Frameworks: Guest-Size-Dependent Isomerization in Cholic Acid Inclusion Crystals with Monosubstituted Benzenes

Kazunori Nakano,[b] Kazuki Sada,*[a] Yukio Kurozumi,[a] and Mikiji Miyata*[a]

Abstract: The crystal structures of inclusion compounds of cholic acid (**CA**) with 28 monosubstituted benzenes have been systematically investigated. All of the crystals belong to the monoclinic space group $P2_1$ and have bilayer structures with one-dimensional molecular channels that can include guest compounds. They are classified into four types of host frameworks that depend on the conformations and stacking modes of the host compound. The host frameworks and the host–guest ratios depend primarily on the molecular volumes of the guest compounds. The packing coefficient of the host cavity (PC_{cavity}), which is the volume ratio of the guest compound to the host cavity, is used to clarify the relationship between the guest volume and isomerization of the host frameworks. The value of PC_{cavity} for stable inclusion compounds lies in the range of 55–70%. Compounds out of this range induce isomerization of the host frameworks. The packing coefficients of other host–guest compounds, in which the guest components are included in the host cavities through steric dimensions and van der Waals forces, are also in this range. These results indicate that PC_{cavity} is a useful parameter correlation for guest recognition and isomerization of the host frameworks.

Keywords: cholic acid · host–guest systems · inclusion compounds · molecular recognition · packing coefficients

Introduction

It is well known that steric complementation between host cavities and guest components is required to form host–guest compounds as a result of a key-and-lock mechanism in molecular recognition. In particular, the size of the included components plays a primary role in the inclusion of guest molecules in the open host frameworks.[1] Qualitatively, the guest compounds that just fit into the steric dimensions of the host cavities are included, while larger or smaller compounds are not included. However, there have been few reports concerned with quantitative analyses and estimations of the size of the host cavities and the guest compounds. Recently, Rebek, Jr. and Mecozzi[2] estimated the volumes and introduced the term packing coefficients of the host cavities (PC_{cavity}), which is defined as the ratio between the molecular volume of the guest component included in the host cavity and the volume of the void in the host cavity, as the parameter to estimate the steric fit between the host and the guest. According to molecular mechanics calculations, a value for PC_{cavity} of 0.55 ± 0.1 gives the best binding constants for the resulting host–guest complexes. However, in the crystalline state, there have been no reports that have attempted to understand the guest inclusions by PC_{cavity}. Only molecular volumes have been used in discussions on the specific reactions or guest recognitions in the solid state.[3, 4] For example, Ohashi and co-workers revealed that photoisomerization of ligands in a series of cobaloxime complexes is controlled by the molecular volumes of the reaction cavities.[3] Gerdil used molecular volumes to rationalize optical resolution and isomerization of *trans*-stilbene in the host frameworks of tri-*o*-thymotide.[4] Therefore, investigations of PC_{cavity} of lattice inclusion crystals would confirm that the size of the guest compounds plays an important role in the formation of the inclusion crystals as well as in the guest-dependent isomerization of the open host frameworks.

Recently, many attempts to design robust nanoporous host frameworks in the crystalline state have been developed with host molecules which have multiple and divergent functional groups that use hydrogen bonding to form the connectiv-

[a] Dr. K. Sada, Y. Kurozumi, Prof. M. Miyata
Department of Material and Life Science
Graduate School of Engineering, Osaka University
2-1 Yamadaoka, Suita, Osaka 565-0871 (Japan)
Fax: (+81) 6879-7404
E-mail: sadakazu@chem.eng.osaka-u.ac.jp
miyata@chem.eng.osaka-u.ac.jp

[b] K. Nakano
Nagoya Municipal Industrial Research Institute, 3-4-41 Rokuban
Atsuta-ku, Nagoya 456-0058 (Japan)

Supporting information for this article is available on the WWW under http://www.wiley-vch.de/home/chemistry/ or from the author.

  0947-6539/01/0701-0209 $ 17.50+.50/0

ities.[5] However, molecular design of the host cavities in the crystalline state is still difficult because of the inability to predict and control the crystal structures.[6] Moreover, isomerization of the open host frameworks has been widely accepted as a substantial property of organic host compounds. The discovery dates back to the 1950's, soon after the structural confirmation of the organic clathrate compounds of tri-*o*-thymotide.[7] Since then many host compounds have been reported with open host frameworks that are dependent on the guest sizes, shapes, and functional groups.[8–15] However, most of the structural investigations have focused on a variety of the host frameworks with a few guest components that have different steric dimensions and functional groups. In order to understand the molecular recognition of a host compound, structural characterizations of many different open host frameworks as well as investigations of the scope and limitations of the guest incorporation are required. Advances in rapid X-ray structural analyses and computer graphic software for the visualization of crystal structures enable us readily to investigate many crystal structures in a short period. In this report, we describe the investigations of twenty-eight crystal structures of cholic acid (**CA**) inclusion compounds with a series of monosubstituted benzenes. To our knowledge, this is the first attempt to understand molecular recognition of the host compound by means of various crystal structures. **CA** is a commercially available steroidal bile acid and has an unusual facially amphiphilic molecular structure. All three hydroxy groups are directed towards the steroidal α-face to form a hydrophilic face and two methyl groups are directed towards the β-face to form a lipophilic face. Recently, the face-differentiating molecular structure has attracted much attention as a molecular scaffold for artificial receptors or combinatorial chemistry.[16] On the other hand, molecular complexes with small alcohols as guests have been known since 1885 in the crystalline state, and a crystallographic study revealed that the guest alcohols are included in a cage-type host cavity.[17, 18] More recently, we found that **CA** includes a wide range of organic compounds, mostly with 1:1 host:guest ratios and that they form bilayer-type structures constructed from hydrogen bonds between the hydrophilic faces and van der Waals associations between the lipophilic faces.[15, 19–22] The guest compounds are entrapped by van der Waals forces and steric complementation in a one-dimensional host cavity, that is, a molecular channel in the lipophilic layer. Further extensive studies reveal that **CA** has at least nine distinguishable host frameworks depending on the guest compounds.[15a] In the bilayer structures, four basic types of host frameworks have been characterized on the basis of conformational isomerization of the side chain and stacking modes in the lipophilic layers. They contain identical host–host hydrogen-bond networks and the lipophilic host channels with slightly different steric dimensions. Therefore, we believe that **CA** would be a suitable host compound to investigate the role of steric fitting between the guest components and the host cavities for guest-dependent isomerization of the host frameworks. Moreover, **CA** is commercially available and relatively cheap, which enables us to try repeated recrystallizations from various organic compounds on a large scale. In this report, we describe systematic investigations of the host frameworks of **CA** to clarify the steric factors of guest incorporations and guest-dependent isomerization of the host frameworks.

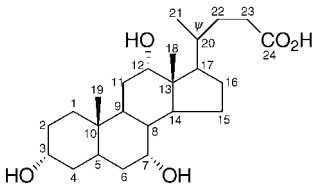

Cholic Acid (**CA**)

Abstract in Japanese:

我々は、コール酸包接化合物の結晶構造を系統的に調べ、ホスト分子が形成する集合様式とゲスト分子との関係を明らかにした。一置換ベンゼンを包接したコール酸結晶はすべて二重層状構造を形成し、親油層にチャンネル状の包接空間を有することが分かった。この際のホスト分子の集合様式は4つのタイプに分けることが出来るが、主にゲストの体積に応じて集合様式が決められていることが分かった。さらに、ホスト分子が形成する空間の体積に対しゲスト分子の体積が占める割合を計算すると55～70％であり、この範囲を超えないよう集合様式やホスト:ゲスト比が調節されていることが分かった。このようなゲスト分子の占有率は、ホストゲスト間に特別な相互作用がない限り他の包接化合物においても同様な値が得られ、今後ゲスト依存的な多形現象の指標としてだけでなく新たなホスト分子の設計の指標としても広く応用できると考えられる。

Results and Discussion

Formation of inclusion crystals and bilayer structures of CA: Table 1 shows monosubstituted benzenes included by **CA**. The host–guest ratios and the crystallographic parameters are summarized in Tables 2 and 3, respectively. Figures 2–5 (see later) illustrate the crystal structures viewed down along crystallographic *b* axis. A common feature found in the crystal structures is a bilayer structure with alternate stacking of lipophilic layers and hydrophilic layers. The facially amphiphilic molecular structure of **CA** gives rise to the bilayer structure by means of van der Waals association of the lipophilic faces and hydrogen bonding between the hydrophilic faces.[15a] The rigid molecular shape makes the layer corrugated, and the offset stacking of the lipophilic faces yields one-dimensional host channels in the lipophilic layers.

All the crystal structures, except that with **57** ($C_6H_5CH_2OH$), contain identical host–host hydrogen-bond

0947-6539/01/0701-0210 $ 17.50+.50/0 *Chem. Eur. J.* **2001**, *7*, No. 1

Table 1. Monosubstituted benzenes that form inclusion compounds with cholic acid (**CA**).

Compound	R	Compound	R	Compound	R
1	H	**21**	C(=O)H	**41**	$CH_2CO_2CH_3$
2	CH_3	**22**	$C(=O)CH_3$	**42**	$CH_2CO_2CH_2CH_3$
3	CH_2CH_3	**23**	$C(=O)CH_2CH_3$	**43**	$OCOCH_3$
4	$CH=CH_2$	**24**	$C(=O)(CH_2)_2CH_3$	**44**	$OCOCH_2CH_3$
5	C≡CH	**25**	$C(=O)CH(CH_3)_2$	**45**	CH_2OCOH
6	$(CH_2)_2CH_3$	**26**	$C(=O)(CH_2)_3CH_3$	**46**	CH_2OCOCH_3
7	$CH_2CH=CH_2$	**27**	$C(=O)(CH_2)_4CH_3$	**47**	$CH_2OCOCH_2CH_3$
8	$C(CH_3)=CH_2$	**28**	$C(=O)C_6H_5$	**48**	$CH_2OCOC(CH_3)=CH_2$
9	$(CH_2)_3CH_3$	**29**	$(CH_2)_2C(=O)CH_3$	**49**	$CH_2OCO(CH_2)_2CH_3$
10	$CH_2CH(CH_3)_2$	**30**	CO_2CH_3	**50**	OCH_3
11	$(CH_2)_4CH_3$	**31**	$CO_2CH_2CH_3$	**51**	OCH_2CH_3
12	$(CH_2)_5CH_3$	**32**	$CO_2(CH_2)_2CH_3$	**52**	OC_6H_5
13	C_6H_{11}	**33**	$CO_2CH(CH_3)_2$	**53**	$OCH_2C_6H_5$
14	$CH_2C_6H_5$	**34**	$CO_2(CH_2)_3CH_3$	**54**	CH_2OCH_3
15	F	**35**	$CO_2CH_2CH(CH_3)_2$	**55**	C≡N
16	Cl	**36**	$CO_2C(CH_3)_3$	**56**	OH
17	Br	**37**	$CO_2(CH_2)_4CH_3$	**57**	CH_2OH
18	I	**38**	$CO_2(CH_2)_2CH(CH_3)_2$	**58**	NH_2
19	CH_2Cl	**39**	$CO_2(CH_2)_5CH_3$	**59**	$NHCH_3$
20	CH_2Br	**40**	$CO_2C_6H_5$	**60**	$NHCH_2CH_3$
				61	NO_2

networks, irrespective of the chemical properties of the guest compounds. Figure 1a shows the hydrogen-bond network of **CA** with **1** as a typical example. The cyclic hydrogen bond network enables the arrangement of the host molecules into a two-dimensional array. The hydroxyl group of **57** is inserted into the cyclic host–host hydrogen-bond network, while the amino group of **58**[20a, 21a] forms weak hydrogen bonds with the hydroxy groups of the host molecules (Figure 1b,c). Unfortunately, disorder of the guest **56** in the host cavity is so severe that we could not investigate the orientations of the guest component accurately. However, the hydroxyl group of **56** probably forms a guest-to-host hydrogen bond in a similar manner to **58**.

Classification of host frameworks: The bilayer structures are robust, common structural motifs of the **CA** inclusion crystals. These crystals are classified into four subtypes based on two conformations (*gauche* and *trans*) of the steroidal side chain, and two types of interdigitation of the methyl groups (α and β) in the lipophilic faces.[15a] A combination of the two factors gives the four types; *α-gauche*, *β-trans*, *β-gauche*, and *α-trans*, which are illustrated in Figures 2, 3, 4, and 5, respectively.

Table 2. Host–guest ratios, molecular volumes, and host frameworks of inclusion compounds of **CA**.

R guest	Host–guest ratio	Molecular volume [Å^3]	Host framework	R guest	Host–guest ratio	Molecular volume [Å^3]	Host framework
−H (**1**)	1:1	83.4	*α-gauche*	$-CO_2CH_2CH_3$ (**31**)	2:1	149.0	*α-trans*
−F (**15**)	1:1	88.4	*α-gauche*	$-CH_2CO_2CH_3$ (**41**)	2:1	149.3	*α-trans*
−OH (**56**)	1:1	93.0	*β-trans*	$-CH_2OCOCH_3$ (**46**)	2:1	149.5	*α-trans*
$-NH_2$ (**58**)	1:1	95.8	*α-gauche*	$-OCOCH_2CH_3$ (**44**)	2:1	149.6	*α-trans*
−Cl (**16**)	1:1	97.5	*α-gauche*	$-CH_2CH(CH_3)_2$ (**10**)	2:1	153.2	*α-trans*
$-CH_3$ (**2**)	1:1	100.8	*α-gauche*	$-(CH_2)_3CH_3$ (**9**)	2:1	153.3	*α-trans*
−Br (**17**)	1:1	101.8	*α-gauche*	$-C(=O)(CH_2)_2CH_3$ (**24**)	2:1	155.9	*α-trans*
−C≡N (**55**)	1:1	102.0	*α-gauche*	$-(CH_2)_2C(=O)CH_3$ (**29**)	2:1	156.3	*α-gauche*
−C(=O)H (**21**)	1:1	104.0	*α-gauche*	$-C(=O)CH(CH_3)_2$ (**25**)	2:1	156.3	*α-trans*
−C≡CH (**5**)	1:1	104.9	*β-gauche*	$-CO_2CH(CH_3)_2$ (**33**)	2:1	165.7	*α-gauche*
−I (**18**)	1:1	107.9	*α-gauche*	$-OC_6H_5$ (**52**)	2:1	166.0	*α-gauche*
$-NO_2$ (**61**)	1:1	109.6	*α-gauche*	$-CH_2CO_2CH_2CH_3$ (**42**)	2:1	166.9	*α-gauche*
$-OCH_3$ (**50**)	1:1	110.4	*α-gauche*	$-CO_2(CH_2)_2CH_3$ (**32**)	2:1	167.0	*α-trans*
$-CH_2OH$ (**57**)	1:1	110.7	*α-trans*	$-CH_2OCOCH_2CH_3$ (**47**)	2:1	167.2	*α-trans*
$-CH=CH_2$ (**4**)	1:1	111.2	*α-gauche*	$-(CH_2)_4CH_3$ (**11**)	2:1	170.6	*α-gauche*
$-NHCH_3$ (**59**)	1:1	113.4	*β-trans*	$-C(=O)(CH_2)_3CH_3$ (**26**)	2:1	173.7	*α-trans*
$-CH_2Cl$ (**19**)	1:1	114.5	*β-trans*	$-CH_2C_6H_5$ (**14**)	2:1	173.9	*α-trans*
$-CH_2CH_3$ (**3**)	1:1	117.7	*β-trans*	$-C(=O)C_6H_5$ (**28**)	2:1	176.0	*α-trans*
$-CH_2Br$ (**20**)	1:1	119.1	*β-trans*	$-C_6H_{11}$ (**13**)	2:1	176.2	*α-trans*
$-C(=O)CH_3$ (**22**)	1:1	120.9	*α-gauche*	$-CH_2OCOC(CH_3)=CH_2$ (**48**)	2:1	177.4	*α-trans*
$-CH_2OCH_3$ (**54**)	1:1	127.6	*β-trans*	$-CO_2C(CH_3)_3$ (**36**)	2:1	182.5	*α-trans*
$-C(CH_3)=CH_2$ (**8**)	1:1	127.7	*α-gauche*	$-OCH_2C_6H_5$ (**53**)	2:1	183.2	*α-gauche*
$-CH_2CH=CH_2$ (**7**)	1:1	127.9	*β-trans*	$-CO_2(CH_2)_3CH_3$ (**34**)	2:1	184.4	*α-trans*
$-OCH_2CH_3$ (**51**)	1:1	128.1	*β-trans*	$-CO_2CH_2CH(CH_3)_2$ (**35**)	2:1	184.4	*α-gauche*
$-NHCH_2CH_3$ (**60**)	1:1	130.1	*β-trans*	$-CH_2OCO(CH_2)_2CH_3$ (**49**)	2:1	184.7	*α-gauche*
$-OCOCH_3$ (**43**)	1:1	131.0	*β-trans*	$-CO_2C_6H_5$ (**40**)	2:1	186.4	*α-gauche*
$-CO_2CH_3$ (**30**)	1:1	131.5	*β-trans*	$-(CH_2)_5CH_3$ (**12**)	2:1	188.5	*α-gauche*
$-CH_2OCOH$ (**45**)	1:1	131.8	*β-trans*	$-C(=O)(CH_2)_4CH_3$ (**27**)	2:1	191.4	*α-trans*
$-(CH_2)_2CH_3$ (**6**)	1:1	136.0	*β-trans*	$-CO_2(CH_2)_4CH_3$ (**37**)	2:1	201.6	*α-trans*
$-C(=O)CH_2CH_3$ (**23**)	1:1	138.9	*β-trans*	$-CO_2(CH_2)_2CH(CH_3)_2$ (**38**)	2:1	201.9	*α-trans*
				$-CO_2(CH_2)_5CH_3$ (**39**)	2:1	219.9	*α-trans*

  0947-6539/01/0701-0211 $ 17.50+.50/0

Table 3. Lattice parameters and dihedral angles for 1:1 inclusion compounds of **CA**.

	Space group	a[Å]	b[Å]	c[Å]	α[°]	β[°]	γ[°]	V[Å^3]	Ψ[°]	Reference
α-gauche										
benzene (**1**)	$P2_1$	13.63	8.04	14.08		114.3		1406	63	[19d]
fluorobenzene (**15**)	$P2_1$	13.57	8.06	14.10		114.4		1405	62	this work
aniline (**58**)	$P2_1$	13.80	8.07	14.09		116.0		1410	61	[20a, 21a]
chlorobenzene (**16**)	$P2_1$	13.66	8.10	14.03		114.6		1411	60	this work
toluene (**2**)	$P2_1$	13.74	8.04	14.01		114.1		1421	61	this work
bromobenzene (**17**)	$P2_1$	13.69	8.10	14.01		114.6		1413	65	this work
benzonitrile (**55**)	$P2_1$	13.64	8.16	14.03		113.9		1428	58	this work
benzaldehyde (**21**)	$P2_1$	13.57	8.11	14.06		113.7		1417	58	this work
iodobenzene (**18**)	$P2_1$	13.68	8.10	14.09		114.2		1423	61	this work
nitrobenzene (**61**)	$P2_1$	13.58	8.11	14.05		113.5		1418	60	[21a]
anisole (**50**)	$P2_1$	13.57	8.08	14.23		114.7		1417	59	this work
styrene (**4**)	$P2_1$	13.57	8.15	14.24		114.6		1431	60	this work
acetophenone (**22**)	$P2_1$	13.72	8.09	14.23		113.7		1447	58	[19b]
ethyl acetate	$P2_1$	13.67	7.82	14.10		113.5		1382		[21b]
ethyl propionate	$P2_1$	13.57	7.97	14.24		113.5		1411		[21b]
2-fluoroaniline	$P2_1$	13.61	8.15	14.03		113.7		1425		[20d]
4-fluoroaniline	$P2_1$	13.83	8.11	13.99		115.5		1416		[20d]
3,4-difluoroaniline	$P2_1$	13.93	8.14	14.03		115.9		1430		[20d]
4-fluoroacetophenone	$P2_1$	13.54	8.15	14.35		113.3		1456		[20c]
2-fluorobenzyl alcohol	$P2_1$	13.42	8.51	13.98		113.2		1467		[20e]
β-trans										
phenol (**56**)	$P2_1$	12.07	7.92	16.39		111.9		1455	−163	this work
N-methylaniline (**59**)	$P2_1$	12.00	7.96	16.22		111.6		1441	−167	this work
benzyl chloride (**19**)	$P2_1$	12.34	7.82	16.24		111.7		1456	−174	this work
ethylbenzene (**3**)	$P2_1$	12.41	7.83	16.28		111.8		1469	−174	this work
benzyl bromide (**20**)	$P2_1$	12.29	7.83	16.30		111.5		1459	−169	this work
benzylmethyl ether (**54**)	$P2_1$	12.11	7.94	16.24		109.9		1468	−169	this work
allylbenzene (**7**)	$P2_1$	12.43	7.88	16.33		112.1		1483	−173	this work
phenetol (**51**)	$P2_1$	12.11	7.97	16.12		108.5		1475	−171	this work
N-ethylaniline (**60**)	$P2_1$	12.14	7.95	16.14		108.2		1481	−171	this work
phenyl acetate (**43**)	$P2_1$	12.26	7.90	16.67		109.7		1478	−180	this work
benzyl formate (**45**)	$P2_1$	12.09	7.96	16.21		109.7		1468	−169	this work
n-propylbenzene (**6**)	$P2_1$	12.07	7.84	16.25		109.8		1447	−172	[19f]
n-propiophenone (**23**)	$P2_1$	12.30	7.94	16.24		109.2		1499	−170	this work, [22a]
3-fluoroacetophenone	$P2_1$	12.79	7.81	16.17		113.1		1486		[20c]
2-chloroacetophenone	$P2_1$	12.58	7.98	16.05		112.2		1492		[20c]
3-methyl-*N*-nitrosopiperidine	$P2_1$	12.35	7.68	16.36		111.1		1447		[22b]
1,5-dimethyl-*N*-nitrosopiperidine	$P2_1$	12.75	7.88	16.36		112.0		1525		[22b]
4-fluoro-*n*-propiophenone	$P2_1$	16.67	8.15	12.06		113.2		1506		[22a]
β-gauche										
ethynylbenzene (**5**)	$P2_1$	12.26	7.80	15.47		106.8		1417	70	this work
propyl acetate	$P2_1$	16.80	7.88	12.11		118.1		1415		[21b]
isopropyl acetate	$P2_1$	16.60	7.98	12.14		117.8		1423		[21b]
α-trans										
benzylalcohol (**57**)	$P2_1$	12.64	8.61	13.90		105.2		1459	−160	this work
acrylonitrile	$P2_1$	12.18	7.88	14.30		104.2		1331		[15c]
methacrylonitrile	$P1$	12.53	14.16	8.28	90.9	94.9	107.2	1396		[15d]
γ-valerolactone	$P2_1$	13.01	8.00	14.05		104.8		1414		[19c]
4-fluorobenzyl alcohol	$P2_1$	12.63	8.61	13.81		105.2		1449		[20e]
methyl acetate	$P1$	12.22	8.19	14.20	90.2	105.7	94.0	1364		[21b]
methyl acetate+isopropyl acetate	$P1$	12.29	8.24	14.25	90.4	105.8	95.0	1382		[21e]
acetone+*o*-dichlorobenzene	$P1$	12.47	8.25	14.21	91.1	106.3	94.4	1399		[21e]
N-nitrosopiperidine	$P2_1$	13.27	7.91	13.82		106.0		1394		[22b]

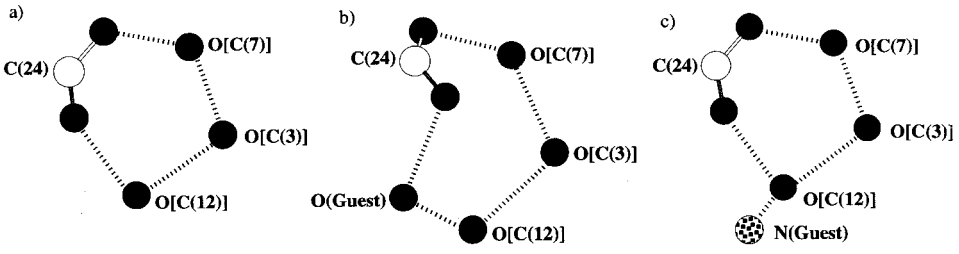

Figure 1. Hydrogen-bond networks of **CA** with a) **1**, b) **57**, and c) **58**. The carbon, nitrogen, and oxygen atoms are represented by open, dotted, and filled circles, respectively.

0947-6539/01/0701-0212 $ 17.50+.50/0 *Chem. Eur. J.* **2001**, *7*, No. 1

α-gauche Type: This host framework (Figure 2) was found as the first example of a channel-type crystal structure of **CA** with **22** in 1988.[19b] Since this discovery, some monosubstituted benzenes, such as **1**,[19d] **58**,[20a, 21a] **61**[21a], and other compounds[20b–e, 21b] have been reported to give this type. The dihedral angles of the side chain at C(17)-C(20)-C(22)-C(23) (ψ) are between 58° and 65°. This conformation refers to the *gauche* type. In the lipophilic layers, the methyl carbon C(18) in the upper layer is located between the methyl carbons C(18) and C(19) of the opposite layer. The stacking is of the α-type. Therefore, this host arrangement is classified as α-*gauche*. In addition nine compounds with the aromatic guest compounds **2**, **4**, **15**, **16**, **17**, **18**, **21**, **50**, and **55** (reported herein) are included in this type. The crystallographic parameters of all of these host-guest compounds are in a narrow range: $13.565 < a < 13.801$ Å, $8.038 < b < 8.164$ Å, $14.011 < c < 14.235$ Å, $113.52 < \beta < 116.01°$, and $1405.4 < V < 1446.7$ Å^3.

β-trans Type: The torsion angles ψ are in the range from $-167°$ to $-180°$. This conformation refers to the *trans* type (Figure 3). In the lipophilic layers, the methyl carbon C(19) in the upper layer is located between the methyl carbons C(18)

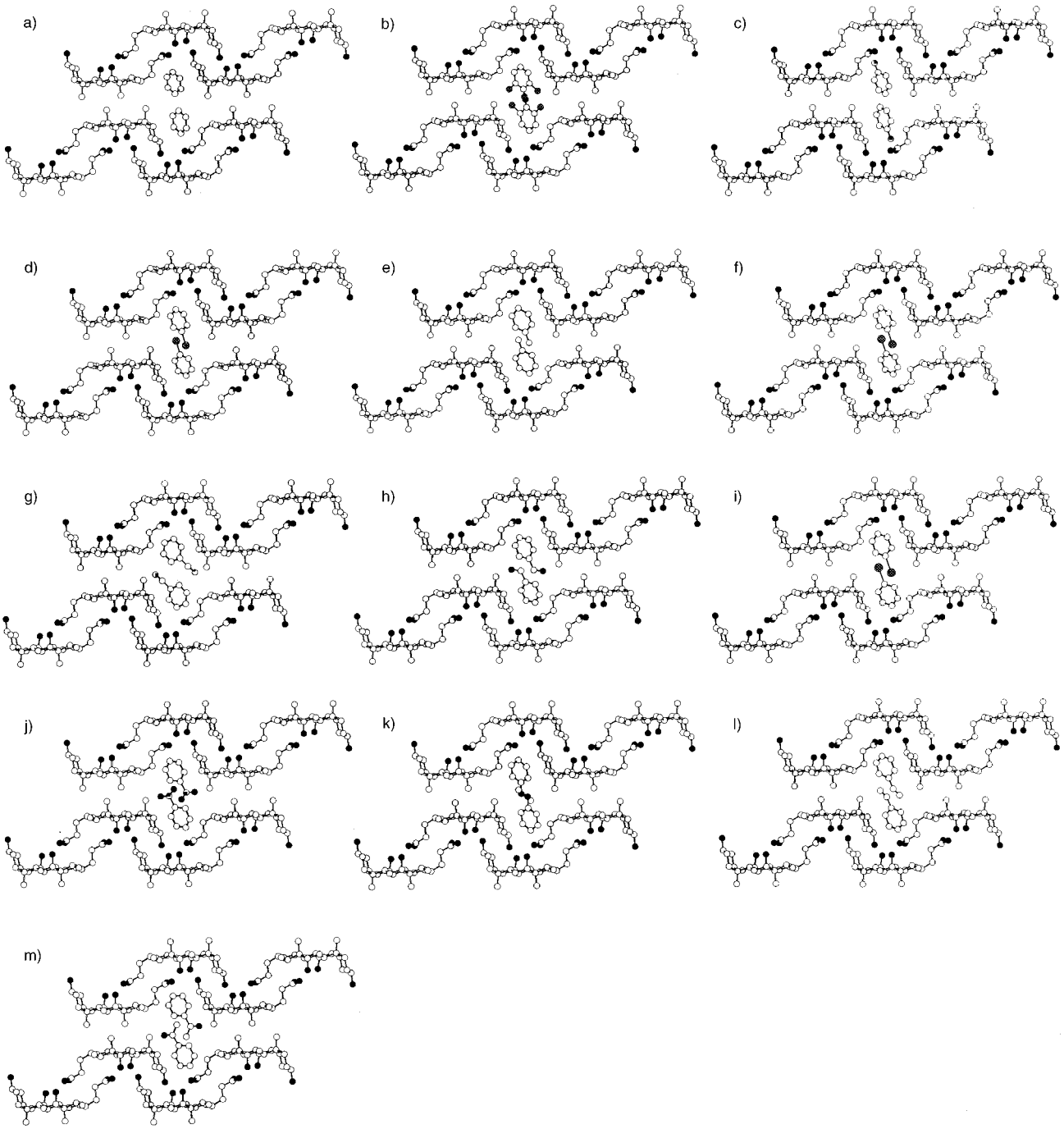

Figure 2. Molecular packing diagrams of *α-gauche* type inclusion crystals of **CA** with a) **1**, b) **15**, c) **58**, d) **16**, e) **2**, f) **17**, g) **55**, h) **21**, i) **18**, j) **61**, k) **50**, l) **4**, and m) **22**. The figures are viewed down along the crystallographic *b* axis. The carbon, nitrogen, oxygen, halide atoms are represented by open, dotted, filled, and shadowed circles, respectively.

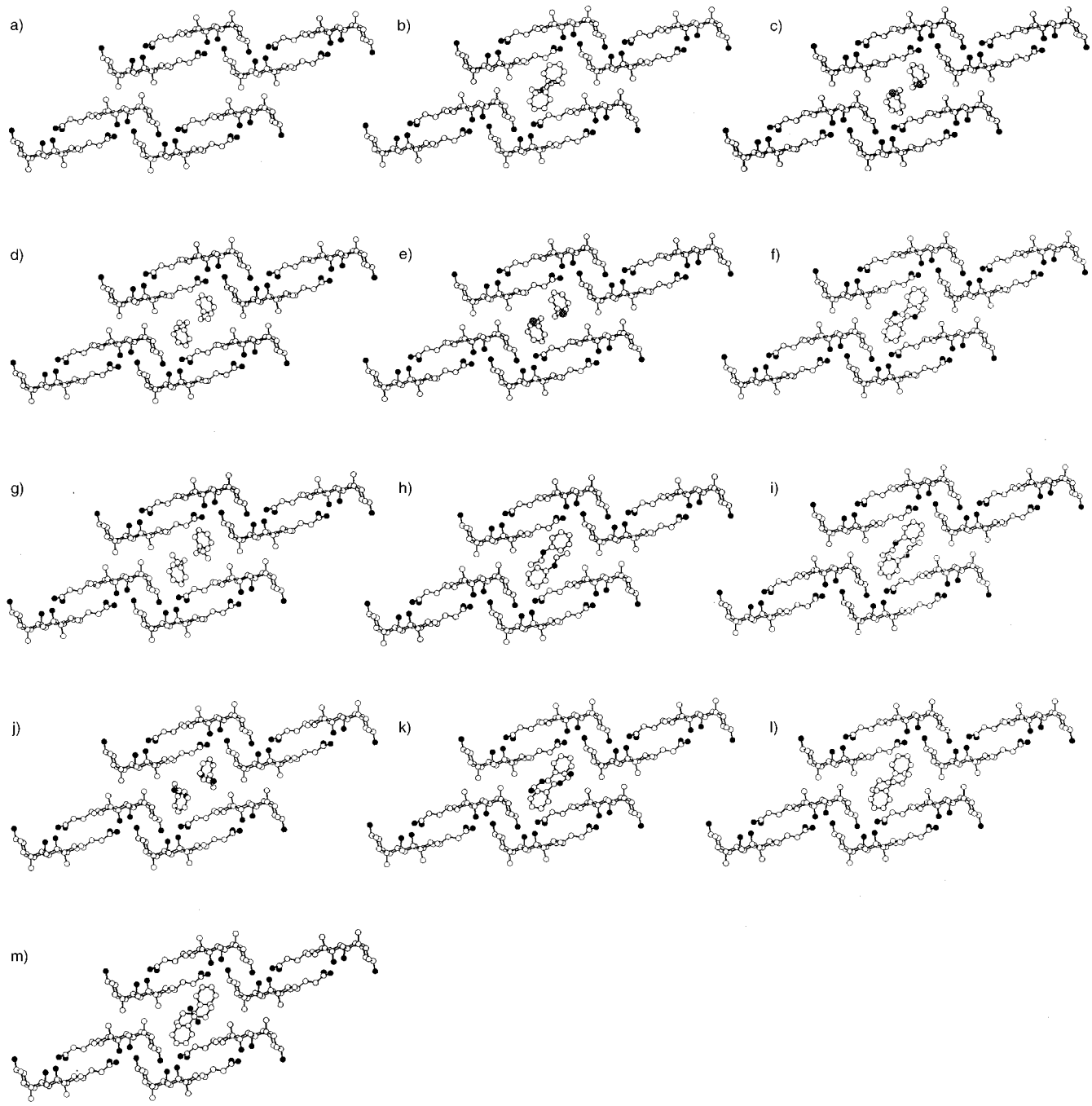

Figure 3. Molecular packing diagrams of *β-trans* type inclusion crystals of **CA** with a) **56**, b) **59**, c) **19**, d) **3**, e) **20**, f) **54**, g) **7**, h) **51**, i) **60**, j) **43**, k) **45**, l) **6**, and m) **23**. The figures are viewed down along the crystallographic *b* axis. The carbon, nitrogen, oxygen, halide atoms are represented by open, dotted, filled, and shadowed circles, respectively.

and C(19) of the opposite layer. This is *β*-type stacking. Sliding of the upper layer of the *α*-type stacking by $\approx$4.5 Å gives the *β*-type stacking. This host framework already has been reported in the crystal structures of **CA** with other aliphatic compounds.[20c, 22a, 22b] Thirteen aromatic compounds (**3**, **6**, **7**, **19**, **20**, **23**, **43**, **45**, **51**, **54**, **56**, **59**, and **60**) are included in this host framework. Regardless of the guest species, the lattice parameters of the *β-trans* type are also within a narrow range; $12.001 < a < 12.434$ Å, $7.821 < b < 7.965$ Å, $16.118 < c < 16.671$ Å, $108.194 < \beta < 112.060^\circ$, and $1441.3 < V < 1498.8$ Å^3.

β-gauche Type: From our current study of aromatic guests, only guest **5** affords the *β-gauche* type structure in the **CA** host–guest compound (Figure 4). The torsion angle of the side chain is 70°, which corresponds to the *α-gauche* type. The interdigitation of the methyl groups in the lipophilic layer is same as the *β-trans* type. This type of structure, however, is known in the crystal structures of **CA** with aliphatic esters.[21b]

α-trans Type: From our current study of aromatic guests, only guest **57** affords a 1:1 *α-trans* type of conformation (Figure 5). The torsion angle is -160°, which corresponds to the *trans* type.

0947-6539/01/0701-0214 $ 17.50+.50/0 *Chem. Eur. J.* **2001**, *7*, No. 1

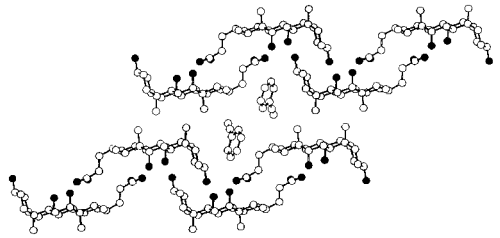

Figure 4. Molecular packing diagram of a *β-gauche* type inclusion crystal of **CA** with **5**. The figure is viewed down along the crystallographic *b* axis. The carbon and oxygen atoms are represented by open and filled circles, respectively.

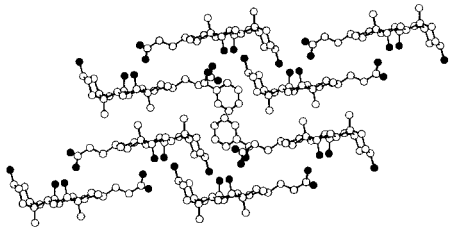

Figure 5. Molecular packing diagram of a *α-trans* type inclusion crystal of **CA** with **57**. The figure is viewed down along the crystallographic *b* axis. The carbon and oxygen atoms are represented by open and filled circles, respectively.

The interdigitation of the methyl groups in the lipophilic side is the *α*-stacking. Since the X-ray crystallographic study of the inclusion compounds of **CA** with *γ*-valerolactone,[19c] there have also been reports that some aliphatic compounds also afforded this host framework, which is further classified into two crystal systems; monoclinic[15c, 20e, 22b] and triclinic.[15d, 21b, 21e]

Sizes and shapes of host cavities: The crystal structures of the host frameworks are affected by the guest compounds. However, differences between the lattice parameters of the *α-gauche* or the *β-trans* type are within only 3%. This indicates that the size and the shape of the host cavities are essentially identical within the same host framework, regardless of the functional groups or the steric dimensions of the guest components. Variations of the host channels only originate from the four types of host architectures. Namely, **CA** can provide at least four different host cavities to include the monosubstituted benzenes by isomerization of the host framework. Table 4 summarizes the free volumes of the host cavities in a unit cell, calculated by Cerius^2.[23] The mean values of the host cavities in the unit cell of the *α-gauche* and *β-trans* type are 330 ± 14 Å^3 and 392 ± 11 Å^3, respectively, when the volumes of the host cavities were calculated by means of a 0.7 Å radius probe. The difference in volume is 62 Å^3, which is similar to the volume difference calculated with a 1.0 Å radius probe.[24] The free volumes of **CA** with **5** in the *β-gauche* host framework and with **57** in the *α-trans* framework are 351 Å^3 and 354 Å^3, respectively. Therefore, the order of the volumes is as follows: *α-gauche* < *α-trans* and *β-gauche* < *β-trans*. The *β-trans*-type host frameworks have the largest host cavities of the **CA** host.

Figures 6 and 7 illustrate the cross-sectional views sliced perpendicular to or parallel to the axis of the channel at the

Table 4. Molecular volume, cavity volume, packing coefficient, length, and thickness of guest molecules.

Guest	Molecular volume [Å^3]	V_{cavity}[a] [Å^3]	PC_{cavity}[b] [%]	$PC_{crystal}$[c] [%]	*l* [Å]	*th* [Å]
α-gauche						
−H (**1**)	83.4	298.1	56.0	71.6	7.4	3.4
−F (**15**)	88.4	319.2	55.4	71.0	7.9	3.4
$-NH_2$ (**58**)	95.8	336.0	57.0	70.5	8.1	3.4
−Cl (**16**)	97.5	327.6	58.0	72.0	8.5	3.5
$-CH_3$ (**2**)	100.8	334.5	60.3	71.3	8.2	4.3
−Br (**17**)	101.8	318.9	63.8	72.4	8.9	3.7
−C≡N (**55**)	102.0	328.4	62.1	72.8	9.2	3.4
−C(=O)H (**21**)	104.0	331.0	62.8	72.5	8.7	3.4
−I (**18**)	107.9	351.6	61.4	72.3	9.1	4.0
$-NO_2$ (**61**)	109.6	326.4	67.2	73.9	8.7	3.4
$-OCH_3$ (**50**)	110.4	332.0	66.5	72.6	9.5	4.3
$-CH=CH_2$ (**4**)	111.2	345.7	64.3	71.7	9.7	3.4
$-C(=O)CH_3$ (**22**)	120.9	344.9	70.1	73.9	9.6	4.3
β-trans						
−OH (**56**)	93.1	390.0	47.7	[d]	8.0	3.4
$-NHCH_3$ (**59**)	113.4	373.7	60.7	72.1	9.6	4.3
$-CH_2Cl$ (**19**)	114.5	370.1	61.9	71.2	9.0	5.1
$-CH_2CH_3$ (**3**)	117.7	386.1	61.0	70.8	9.5	4.9
$-CH_2Br$ (**20**)	119.1	400.4	59.5	71.6	9.2	5.3
$-CH_2OCH_3$ (**54**)	127.6	398.6	64.0	71.8	10.0	5.2
$-CH_2CH=CH_2$ (**7**)	127.9	393.9	64.9	72.4	9.5	5.8
$-OCH_2CH_3$ (**51**)	128.1	389.2	65.8	72.2	11.0	4.3
$-NHCH_2CH_3$ (**60**)	130.1	406.8	64.0	71.4	11.0	4.3
$-OCOCH_3$ (**43**)	131.0	399.4	65.6	71.6	10.0	5.5
$-CH_2OCOH$ (**45**)	131.8	387.7	68.0	72.5	11.0	5.4
$-(CH_2)_2CH_3$ (**6**)	136.0	387.2	70.2	73.7	10.0	5.1
$-C(=O)CH_2CH_3$ (**23**)	138.9	407.5	68.2	73.5	11.0	4.3
β-gauche						
−C≡CH (**5**)	104.9	351.1	59.8	71.5	10.0	3.4
α-trans						
$-CH_2OH$ (**57**)	110.7	354.0	62.5	70.6	8.7	5.2

[a] V_{cavity} is the volume of the cavity in the unit cell calculated with a 0.7 Å radius probe. [b] PC_{cavity} is the packing coefficient of the guest components in the host cavity: PC_{cavity} = (molecular volume) × 2/V_{cavity} × 100. [c] $PC_{crystal}$ is the packing coefficient of the whole crystal. [d] $PC_{crystal}$ cannot be calculated because of the disorder.

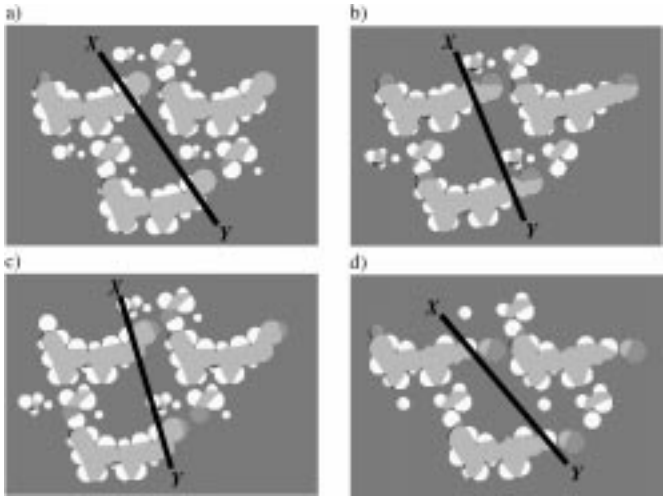

Figure 6. Cross-sections of the host channels sliced perpendicular to the direction of the channel; a) **CA** with **1** as a typical example for *α-gauche* type, b) **CA** with **3** as *β-trans* type, c) **CA** with **5** as *β-gauche* type, and d) **CA** with **57** as *α-trans* type, respectively. The guest molecules are omitted. Carbon, hydrogen, and oxygen atoms are represented in white, gray, and black, respectively. The bold line along *X* – *Y* indicates the position sliced parallel to the direction of the channel which is shown in Figure 7.

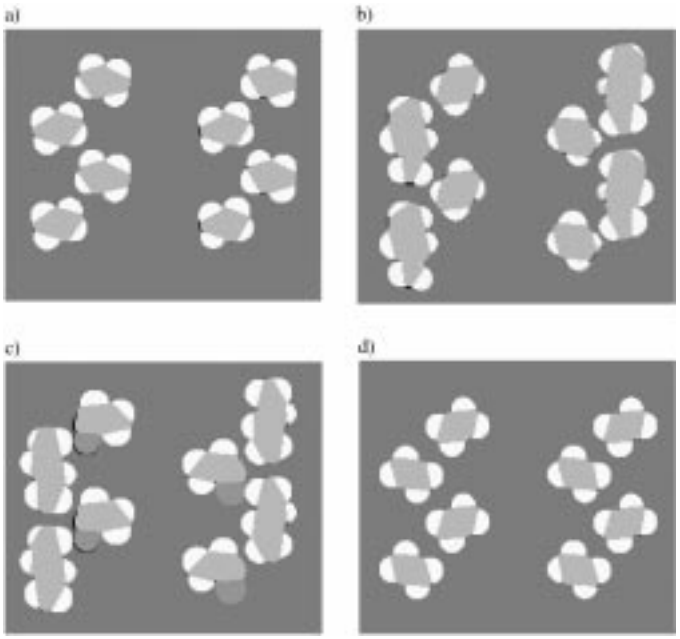

Figure 7. Cross-sections of the host channels sliced parallel to the direction of the channel; a) **CA** with **1** as a typical example for *α-gauche* type, b) **CA** with **3** as *β-trans* type, c) **CA** with **5** as *β-gauche* type, and d) **CA** with **57** as *α-trans* type, respectively. The guest molecules are omitted. Carbon, hydrogen, and oxygen atoms are represented in gray, white, and black, respectively.

same positions. The perpendicular cross-sections of *α-gauche*, *β-trans*, *β-gauche*, and *α-trans* are nearly elliptical, large elliptical, distorted round, and round, respectively. The parallel cross-sections permit us to clarify the difference of the shapes between the *gauche* and the *trans* types. The host cavities in the *α*- and *β-gauche* types have square grooves, while those in the *α*- and *β-trans* types have triangular grooves.

Size-dependent isomerization of host frameworks: Most of the monosubstituted benzenes are incorporated in two common types, *α-gauche* and *β-trans*. The size of the guest compounds contribute to isomerization of the host framework. The smaller guests in the range of 83.4 – 127.7 Å^3 prefer the *α-gauche* type and the larger guests in the range of 93.0 – 138.9 Å^3 tend to form the *β-trans* type (Table 2). This is a good agreement with the fact that the *β-trans* host framework has a 119 % larger cavity than the *α-gauche* framework. When the molecular volumes of the guest compounds exceed the upper limit of the *β-trans* type, 140 Å^3, the host – guest ratios change from 1:1 to 2:1 and simultaneously the host frameworks isomerize from the *β-trans* type to the *α* types. As the *α* types have smaller cavities than *β-trans*, and the number of guest components in the unit cell is reduced. Both of the host frameworks and the host – guest ratios change with an increase in guest volume in the order, *α-gauche* lattice at 1:1 stoichiometry < *β-trans* lattice at 1:1 stoichiometry < *α-gauche* or *α-trans* lattice at 2:1 stoichiometry. This indicates that the guest-dependent isomerization of the host frameworks as well as the change of the host – guest stoichiometries enable **CA** to include a variety of monosubstituted benzenes.

Shape-dependent isomerization of host frameworks: The volumes of the guest compounds play a primary role for the isomerization of the host frameworks. Small and large guest compounds are included in the *α-gauche* or the *β-trans* type, respectively. However, it is possible to incorporate the medium-size guests (93.0 – 127.7 Å^3) in both of the host lattices. In these cases, the shape of the guest compounds determine the host frameworks. To specify the shapes, we introduce two parameters: length of the longitudinal molecular axis *l*, and thickness of the guest molecules, *th* (Figure 8). They are estimated based on geometrical calculations from the molecular models (Table 4).

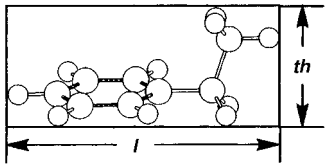

Figure 8. Length (*l*) and thickness (*th*) of guest molecules were defined from molecular modeling.

The guest compounds included in the *α-gauche* type have $l < 9.7$ Å and $th < 4.3$ Å, while those in the *β-trans* type have $l > 9.0$ Å and $th > 4.3$ Å, except for **56**. This means that the shorter and thinner molecules prefer to form the *α-gauche* lattice, while longer and thicker molecules prefer the *β-trans* lattice. For example, **50** and **3** have similar volumes and *l* on account of the similar size of the substituent groups. However, *th* of the former is smaller than that of the latter, because the torsion angle between the terminal methyl group and the phenyl ring in the former guests is 0°, but in the latter it is 90°. The difference between the thicknesses gives the different host frameworks. When the molecular volumes are in the boundary between two host frameworks, the shape determines the host frameworks. Furthermore, the characteristic shapes of **5** and **57** give an explanation of the two less common types. The length ($l = 10.0$) of **5** is too large to be incorporated in the *α-gauche* lattice, but the volume is too small for it to be incorporated in the *β-trans* lattice. It prefers the unique cavity of the *β-gauche* lattice. The center of the cavity is narrowed because of the *gauche* conformation of the side chain. The acetylene moiety just fits into the narrow corridor, as shown in Figure 6c. For guest **57**, the thickness ($th = 5.2$ Å) is beyond the range in the *α-gauche* framework (3.4 Å < *th* < 4.3 Å), and the volume is too small for the *β-gauche* lattice. Therefore, the molecular shape and the hydroxyl group of **57** contribute to the formation of the *α-trans* type. Molecule **56** is an exceptional guest. In spite of the small volume (93.1 Å^3) and the short thin molecular shape ($l = 8.0$ Å, $th = 3.4$ Å), it has a *β-trans* type host. Unfortunately, even at low temperatures, we could not confirm the orientation of the guest compound in the host cavity because of the disorder of the phenyl ring, while the host framework was found to be of the *β-trans* type. The disorder can be understood by the fact that the size of the guest molecule is too small for the host cavity. The host – guest hydrogen bonding between **56** and the host compound may force the guest molecule to arrange in the specific direction in the larger host cavity.

0947-6539/01/0701-0216 $ 17.50+.50/0 *Chem. Eur. J.* **2001**, *7*, No. 1

Packing coefficients of host cavities: In order to understand the size-dependent isomerization and the guest recognition of **CA**, the estimations of the steric fit between the host cavities and guest components are required. We used the packing coefficients of the host cavities (PC_{cavity}) as a parameter for the steric fit of the guest component into the host cavity. This parameter is calculated from the free volume of the host cavities and the molecular volume of the guest compounds in the unit cell. Table 4 summarizes the PC_{cavity} of all the examined inclusion crystals, together with $PC_{crystal}$, the ratios between the volumes of the unit cell and the molecular volumes of all components in the unit cell. PC_{cavity} of the *α-gauche* and *β-trans* host cavities, except for the complex with **56**, is statistically distributed in the ranges $62 \pm 5\%$ and $65 \pm 3\%$, respectively. The similar values found for each host framework indicate that PC_{cavity} is independent of the shape and size of the host frameworks. In a series of guest compounds included in the same host frameworks, PC_{cavity} tends to increase with increasing guest volume, because the volumes of the host cavities are less sensitive than those of the guest molecules. Guests with packing coefficients of $>70\%$ do not form stable inclusion crystals; they induce isomerization to another host framework that has a larger host cavity or/and reduce the host-to-guest ratios. This is because close packing gives rise to steric repulsion between the host molecules and the guest components and restrictions in the freedom of motion of the guest components in the host cavities. On the other hand, guests with packing coefficients of $<55\%$ also do not form the inclusion crystals and induce isomerization to another host framework that has smaller host cavities. Therefore, the optimal values PC_{cavity} (55–70%) should be required to form the stable inclusion compounds, particularly when the guest components are entrapped in the host cavities by the steric dimensions and van der Waals forces. These results indicate that PC_{cavity} is a good parameter for the estimation of the steric fit and plays an important role in the formation of the host–guest compounds, the host–guest ratios, and the isomerization of the host frameworks. On the other hand, guest **56**, which has a hydrogen-bonding functional group, has the lowest PC_{cavity} (48%). The size of the guest components is small; however, the host framework is the biggest. This steric misfit decreases the packing coefficient of **56**. The host–guest hydrogen bonding would hold the guest molecule within the relatively large host cavity. Therefore, additional strong intermolecular interactions, such as π–π interactions and hydrogen bonds, between a host cavity and a guest compound expand the range of PC_{cavity}. Since there have been many examples of the host–guest compounds in crystalline state, we performed the calculation of PC_{cavity} of the selected host–guest compounds that have one-dimensional host channels without any host–guest hydrogen bonds, as shown in Table 5. The packing coefficients of the host cavities are in the range of those observed in the host frameworks of **CA**. Larger packing coefficients are reached if

Table 5. Packing coefficients of the selected crystalline inclusion compounds.

Host	Guest	No. of guest molecules in the unit cell	Molecular volume [Å^3]	V_{cavity}[a] [Å^3]	PC_{cavity}[b] [%]	Reference
9-(3,5-dihydroxyphenyl)anthracene	methyl acetate	4	76.9	486.9	63.2	[10]
9-(3,5-dihydroxyphenyl)anthracene	ethyl acetate	4	94.1	551.0	68.3	[10]
9-(3,5-dihydroxyphenyl)anthracene	acetone	4	66.3	440.4	60.2	[10]
9-(3,5-dihydroxyphenyl)anthracene	2-butanone	4	83.5	505.6	66.1	[10]
9-(3,5-dihydroxyphenyl)anthracene	3-pentanone	4	100.8	612.6	65.8	[10]
9-(3,5-dihydroxyphenyl)anthracene	3-hexanone	4	119.0	684.1	69.6	[10]
9-(3,5-dihydroxyphenyl)anthracene	4-heptanone	4	136.1	742.6	73.3	[10]
9-(3,5-dihydroxyphenyl)anthracene	cyclohexanone	4	106.4	605.5	70.1	[10]
9-(3,5-dihydroxyphenyl)anthracene	methyl benzoate	4	131.5	668.5	78.7	[10]
9-(3,5-dihydroxyphenyl)anthracene	isopropyl benzoate	4	165.7	866.7	76.5	[10]
9-(3,5-dihydroxyphenyl)anthracene	isopropyl benzoate	4	165.7	898.1	73.8	[10]
9-(3,5-dihydroxyphenyl)anthracene	acetophenone	4	120.9	668.7	72.3	[10]
9-(3,5-dihydroxyphenyl)anthracene	benzoquinone	4	97.6	547.4	71.3	[10]
9-(3,5-dihydroxyphenyl)anthracene	tetramethylbenzoquinone	4	164.7	804.6	81.9	[10]
9-(3,5-dihydroxyphenyl)anthracene	nitrobenzene	12	109.6	1819.0	72.3	[10]
(guanidinium)$_2$ azobenzene-4,4′-disulfonate	1,4-dibromobenzene	1	119.5	175.9	67.9	[14]
(guanidinium)$_2$ azobenzene-4,4′-disulfonate	1,4-divinylbenzene	1	139.3	189.6	73.5	[14]
(guanidinium)$_2$ 4,4′-biphenyldisulfonate	1,4-dibromobenzene	4	119.5	712.4	67.1	[14]
(guanidinium)$_2$ 4,4′-biphenyldisulfonate	1,4-divinylbenzene	6	139.3	1249	66.9	[14]
(guanidinium)$_2$ 4,4′-biphenyldisulfonate	nitrobenzene	8	109.6	1203	72.9	[14]
(guanidinium)$_2$ 4,4′-biphenyldisulfonate	1-nitronaphthalene	4	153.0	717.3	85.3	[14]
(guanidinium)$_2$ 4,4′-biphenyldisulfonate	naphthalene	1	127.0	149.5	84.9	[14]
1,1′,6,6′,7,7′-hexahydroxy-3,3′-dimethyl-5,5′-diisopropyl-(2,2′-binaphthalene)-8,8′-dicarboxaldehyde	acetone	2	66.3	226.3	58.6	[12]
1,1′,6,6′,7,7′-hexahydroxy-3,3′-dimethyl-5,5′-x diisopropyl-(2,2′-binaphthalene)-8,8′-dicarboxaldehyde	1-butanal	2	84.1	224.5	74.9	[12]
1,1′-binaphthyl-2,2′-dicarboxylic acid	bromobenzene	2	101.8	314.0	64.8	[13b]
1,1′-binaphthyl-2,2′-dicarboxylic acid	*o*-xylene	4	117.6	704.3	66.8	[13a]
1,1′-binaphthyl-2,2′-dicarboxylic acid	*m*-xylene	2	117.8	353.6	66.6	[13a]
1,1′-binaphthyl-2,2′-dicarboxylic acid	*p*-xylene	2	117.5	340.4	69.0	[13a]

[a] V_{cavity} is the volume of the cavity in the unit cell calculated with a 0.7 Å radius probe. [b] PC_{cavity} = (molecular volume) × (number of guest molecule in unit cell)/$V_{cavity} \times 100$.

the compounds are stabilized by $\pi-\pi$ interactions. Unfortunately, the upper and lower limits of PC_{cavity} are not clear because of a lack of systematic structural investigation of each host framework. However, these results indicate that the appropriate PC_{cavity} (55–70%) should be required to form the stable inclusion compounds. These facts suggest that the optimal PC_{cavity} is independent of both the host compounds and the host frameworks. Upper and lower limits of the PC_{cavity} are affected by the interactions between host cavities and guest components.

The behavior of the packing coefficients with respect to the formation of the inclusion crystals is quite similar to those of the tennis-ball-type host compounds in solution.[16] Suitable packing coefficients of the host cavities are required to form stable complexes. Comparison of the absolute value of PC_{cavity} between them may have no sense because an accurate estimation of the host cavities has been never achieved in the solid state nor in solution. However, the range of packing coefficients in the inclusion cavities is smaller than those of organic crystals (66–77%)[6] or protein cores,[25] and slightly larger than those of the calculated results of the encapsulated complexes in the solution (46–64%) or the liquid state (44–56%) (Figure 9).[2] This indicates that guest molecules in the host cavities of lattice inclusion compounds have an intermediate mobility and anisotropy, which corresponds to dynamic properties and selective reactions of guest components in the host cavities.

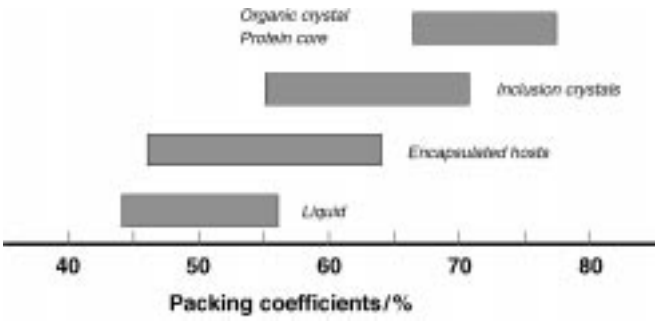

Figure 9. Packing coefficients in various states: organic crystals,[6] protein cores,[25] inclusion crystals, encapsulated hosts,[2] and liquid state.[2]

Conclusions

We have described the systematic structural investigations of inclusion compounds of **CA** with a series of monosubstituted benzenes. The four host frameworks are acquired by a change in the conformation of the side chain and the type of interdigitation between the methyl groups. Each host framework can include a limited range of guest compounds. Moreover, formation of the host–guest compounds, host–guest ratios, and the structures of the host frameworks depend mainly on the volumes of the guest components. This indicates that the spatial fit between the guest components and the host cavities plays a primary role for guest inclusion in the crystalline state, and that the guest compounds act as templates for the host frameworks. In order to clarify the role of the guest volume to enclathration in the crystalline state more precisely, we calculated the packing coefficients of the host cavities of inclusion crystals of **CA** as well as other known host compounds. This is the first application of PC_{cavity} for the correlation of guest recognition in lattice inclusion compounds. The values of PC_{cavity} are statistically distributed in the range of 55–70%, when the guest components are included in the host cavities by van der Waals interactions and steric complementation. The optimal PC_{cavity} should be required to form the stable inclusion crystals, because compounds out of this range give rise to isomerization or collapse of the host frameworks. Moreover, we found that PC_{cavity} is not dependent on the host compounds and the host frameworks. Calculations of the PC_{cavity} of the guest candidates help to predict the boundary of isomerization of the host framework and the host–guest ratio. Guest candidates should be carefully designed to have the appropriate packing coefficients in order to construct the expected host frameworks. On the other hand, the importance of the guest components in the construction of the designed host frameworks has recently been recognized.[5] This means that guest compounds act as a template for host frameworks. Our results support this idea and give us insight into the design of guest components and establishment of the desired host framework. Computer-aided molecular modeling enables us to calculate the void volumes of the host cavity on the basis of the host frameworks designed from the molecular structure. The spatial requirements of the guest components can be estimated from PC_{cavity} and the volumes of the designed host cavity. Therefore, we believe that the packing coefficient will be useful to design and predict host frameworks. This should become the first step for designing the organic host compounds with directed specific guest recognition. Finally, this work indicates that PC_{cavity} of the inclusion compounds is intermediate between the liquid state and the solid state and that packing coefficients can be correlated with mobility and anisotropy of the included components. These results link molecular recognition in the solid state with that in solution.

Experimental Section

General methods: All chemicals and solvents were commercially available and used without any further purification. Infrared spectra were recorded on a JASCO IR-Report-100 or JASCO IR-810 spectrometer. Differential scanning calorimetry (DSC), and thermal gravimetry (TG), were performed on a Rigaku TAS100 system; ≈10 mg samples were heated from 40 to 230 °C at a heating rate of 5 °C min^{-1}. X-ray powder diffraction (XRD) patterns were measured with a Rigaku RINT-1100 diffractometer at room temperature.

Preparation of the inclusion crystals:

Method A: **CA** (100 mg) was dissolved by warming in the liquid guest (usually 2–3 mL), and the resulting solution was allowed to stand at room temperature. The needle-like crystals were collected and dried on the filter paper.

Method B: If **CA** was insufficiently soluble in the liquid guest, 1-butanol was used as a solvent: **CA** (100 mg) was dissolved with warming in 1-butanol (0.4 mL), and the liquid guest (usually 1–2 mL) was poured into the resulting solution. The crystals were isolated in the same manner as in Method A.

Crystal structure determinations: X-ray diffraction data were collected on a Rigaku AFC-7R four-circle diffractometer or a RAXIS-IV diffractometer with a two-dimensional area detector and graphite-monochromatized

0947-6539/01/0701-0218 $ 17.50+.50/0 *Chem. Eur. J.* **2001**, *7*, No. 1

$Mo_{K\alpha}$ radiation. Lattice parameters were obtained by least-squares analysis of 25 reflections measured in the range $20 < 2\theta < 25$ for the four-circle diffractometer and reflections for 3 oscillation images for the area detector. Direct methods (SHELEX86 or SIR92) were used for the structure solution. The structure was refined by the full-matrix least-squares procedure with the program TEXSAN.[26] In the case of **CA · 3**, **CA · 15**, **CA · 17**, **CA · 45**, **CA · 50**, **CA · 51**, **CA · 54**, and **CA · 57**, non-hydrogen atoms of the host compound were refined with anisotropic displacement parameters. The guest molecules were located unambiguously in difference-electron density maps and refined anisotropically with bond length restraints. Hydrogen atoms were placed in idealized positions and were not subjected to further refinement. In the case of **CA · 56**, only the host molecule was refined with anisotropic displacement parameters because the guest molecule was completely disordered. In all the other crystals, all non-hydrogen atoms were refined with anisotropic displacement parameters and hydrogen atoms of the host molecule were placed in idealized positions and refined as riding atoms with the relative isotropic displacement parameters. Hydrogen atoms of the guest molecule were placed in idealized positions and not refined. All calculations were performed with the TEXSAN crystallographic software package.[26] The conditions of measurement and structural details are listed in the Supporting Information (Table II).

Crystallographic data (excluding structure factors) for the structures reported in this paper have been deposited with the Cambridge Crystallographic Data Centre as supplementary publication nos. CCDC-145690 to CCDC-145711. Copies of the data can be obtained free of charge on application to CCDC, 12 Union Road, Cambridge CB21EZ, UK (fax: (+44) 1223 336-033; e-mail: deposit@ccdc.cam.ac.uk).

Molecular graphics: A molecular graphics study was carried out by with the computer software based on MODRASTE.[27] The atomic radii of hydrogen, carbon, and oxygen in the cross-sectional views were fixed at 1.20 Å, 1.60 Å, and 1.45 Å, respectively.

Calculations: The volumes of the host cavities were calculated from the atomic coordinations with the program Free Volume[28] in the Cerius^2 software package (version 4.0).[23] The following values were used for the atomic radii: H = 1.20 Å, C = 1.70 Å, N = 1.65 Å, O = 1.60 Å, F = 1.47 Å, Cl = 1.75 Å, Br = 1.85 Å, I = 1.98 Å. The calculation involves rolling of a spherical probe along the interior surface, but there is no universally accepted radius of the probe. Rebek, Jr. et al. reported that the packing coefficient of 55 ± 9% gives the best binding of the host–guest complex in solution when a 0.7 Å radius probe is used.[2] Rebek also stated that the size of the probe gave rise to a tolerance error range for a larger cavity calculation. We also used the same size probe to calculate the **CA** cavities because all of the cavities have enough volume. The employment of the same size probe would permit the comparison of the cavity volumes and the packing coefficients in solution and the solid state. We wish to emphasize here that the cavity volumes or packing coefficients are not used as absolute values but as relative values for each crystal.

Acknowledgements

This work was supported by Grants-in-Aid for Scientific Research from the Ministry of Education, Science, Sports, and Culture, Japan (Priority Area, Dynamic Control of Stereochemistry) and by the TOKYO OHKA FOUNDATION. We also thank for Prof. Yasushi Kai at Osaka University for use of the Cambridge Crystallographic Data Base.

[1] Reviews: a) S. Ibach, V. Prautzsch, F. Vögtle, *Acc. Chem. Res.* **1999**, *32*, 729–740; b) A. Jasat, J. C. Sherman, *Chem. Rev.* **1999**, *99*, 931–967; c) K. A. Connors, *Chem. Rev.* **1997**, *97*, 1325–1357; d) M. M. Conn, J. Rebek, Jr. *Chem. Rev.* **1997**, *97*, 1647–1668; e) A. Ikeda, S. Shinkai, *Chem. Rev.* **1997**, *97*, 1713–1734; f) *Comprehensive Supramolecular Chemistry*, *Vol. 1–10* (Eds.: J.-M. Lehn, J. L. Atwood, J. E. D. Davies, D. D. MacNicol, F. Vögtle), Pergamon, Oxford, **1996**.

[2] S. Mecozzi, J. Jr. Rebek, Jr., *Chem. Eur. J.* **1998**, *4*, 1016–1022.

[3] a) Y. Ohashi, K. Yanagi, T. Kurihara, Y. Sasada, Y. Ohgo, *J. Am. Chem. Soc.* **1981**, *103*, 5805–5812; b) Y. Ohashi, *Acc. Chem. Res.* **1988**, *21*, 268–274; c) Y. Ohashi in *Reactivity in Molecular Crystals*, Kodansha, Tokyo, **1993**, pp. 115–153; more recently, see d) T. Yamada, Y. Ohashi, *Bull. Chem. Soc. Jpn.* **1998**, *72*, 2527–2537.

[4] a) R. Arad-Yellin, B. S. Green, M. Knossow, G. Tsoucaris, *J. Am. Chem. Soc.* **1983**, *105*, 4561–4571; b) R. Gerdil, *Top. Curr. Chem.* **1987**, *140*, 72–105; c) R. Gerdil, in *Comprehensive Supramolecular Chemistry*, *Vol. 6* (Eds: J. L. Atwood, J. E. D. Davies, D. D. MacNicol, J.-M. Lehn, F. Vögtle, F. Toda, R. Bishop), Pergamon, Oxford, **1996**, pp. 239–280.

[5] Reviews: a) D. D. MacNicol, J. J. McKendrick, D. R. Wilson, *Chem. Soc. Rev.* **1978**, *7*, 66–87; b) J. E. D. Davies, W. Kemula, H. M. Powell, N. O. Smith, *J. Incl. Phenom.* **1983**, *1*, 3–44; c) *Top. Curr. Chem.* **1988**, *140*, whole issue; d) *Top. Curr. Chem.* **1988**, *149*, whole issue; e) *Inclusion Compounds*, *Vol. 1–3* and *4–5* (Eds.: J. L. Atwood, J. E. D. Davies, D. D. MacNicol), Academic Press, London, **1984**, and Oxford Press, Oxford, **1991**; f) *Comprehensive Supramolecular Chemistry*, *Vol. 6* (Eds: J. L. Atwood, J. E. D. Davies, D. D. MacNicol, J.-M. Lehn, F. Vögtle, F. Toda, R. Bishop), Pergamon, New York, **1996**; g) R. Bishop, *Chem. Soc. Rev.* **1996**, 311–319.

[6] For example, see: a) A. I. Kitaigorodskii, *Molecular Crystals and Molecules*, Academic Press, New York, **1973**; b) G. R. Desiraju, *Crystal Engineering: The Design of Organic Solids*, Elsevier, New York, **1989**; c) A. Gavezzotti, *Acc. Chem. Res.* **1994**, *27*, 309–314.

[7] D. Lawton, H. M. Powell, *J. Chem. Soc.* **1958**, 2339–2357.

[8] M. D. Hollingsworth, D. B. Santarsiero, K. D. M. Harris, *Angew. Chem.* **1994**, *106*, 698–701; *Angew. Chem. Int. Ed. Engl.* **1994**, *33*, 649–652.

[9] A. T. Ung, D. Gizachew, R. Bishop, M. L. Scudder, I. G. Dance, D. C. Craig, *J. Am. Chem. Soc.* **1995**, *117*, 8745–8756.

[10] Y. Endo, T. Ezuhara, M. Koyanagi, H. Masuda, Y. Aoyama, *J. Am. Chem. Soc.* **1997**, *119*, 499–505.

[11] M. P. Byrn, C. J. Curtis, Y. Hsiou, S. I. Khan, P. A. Sawin, S. K. Tendick, A. Terzis, C. E. Strouse, *J. Am. Chem. Soc.* **1993**, *115*, 9480–9497.

[12] M. Gdaniec, B. T. Ibragimov, S. A. Talipov, in *Comprehensive Supramolecular Chemistry*, *Vol. 6* (Eds: J. L. Atwood, J. E. D. Davies, D. D. MacNicol, J.-M. Lehn, F. Vögtle, F. Toda, R. Bishop), Pergamon, Oxford, **1996**, pp. 117–145.

[13] a) K. Beketov, E. Weber, J. Seidel, K. Köhnke, K. Makhkamov, B. Ibragimov, *Chem. Commun.* **1999**, 91–92; b) B. Ibragimov, K. Beketov, K. Makhkamov, E. Weber, *J. Chem. Soc. Perkin Trans. 2* **1997**, 1349–1352.

[14] a) V. A. Russell, C. C. Evans, W. Li, M. D. Ward, *Science* **1997**, *276*, 575–579; b) J. A. Swift, A. M. Pivovar, A. M. Reynolds, M. D. Ward, *J. Am. Chem. Soc.* **1998**, *120*, 5887–5897; c) C. C. Evans, L. Sukarto, M. D. Ward, *J. Am. Chem. Soc.* **1999**, *121*, 320–325.

[15] a) M. Miyata, K. Sada, in *Comprehensive Supramolecular Chemistry*, *Vol. 6* (Eds: J. L. Atwood, J. E. D. Davies, D. D. MacNicol, J.-M. Lehn, F. Vögtle, F. Toda, R. Bishop), Pergamon, Oxford, **1996**, pp. 147–176; b) M. Miyata, K. Sada, K. Hirayama, Y. Yasuda, K. Miki, *Supramol. Chem.* **1993**, *2*, 283–288; c) K. Nakano, K. Sada, M. Miyata, *Chem. Commun.* **1996**, 989–990; d) K. Nakano, K. Sada, M. Miyata, *Prog. Colloid Polym. Sci.* **1997**, *106*, 249–251.

[16] a) A. P. Davis, *Chem. Soc. Rev.* **1993**, *22*, 243–253; b) A. P. Davis, R. P. Bonar-law, J. K. M. Sanders in *Comprehensive Supramolecular Chemistry*, *Vol. 4* (Eds.: J. L. Atwood, J. E. D. Davies, D. D. MacNicol, J.-M. Lehn, F. Vögtle, Y. Murakami), Pergamon, Oxford, **1996**, pp. 257–286; c) Y. Li, J. R. Dias, *Chem. Rev.* **1997**, *97*, 283–304; d) P. Wallimann, T. Marti, A. Fürer, F. Diederich, *Chem. Rev.* **1997**, 1567–1608.

[17] P. Latschinoff, *Chem. Ber.* **1885**, *18*, 3039.

[18] a) P. L. Johnson, J. P. Schaefer, *Acta Crystallogr. Sect. B* **1972**, *28*, 3083–3088; b) E. L. Jones, L. R. Nassimbeni, *Acta Crystallogr. Sect. B* **1990**, *46*, 399–405.

[19] a) M. Miyata, M. Shibakami, W. Goonewardena, K. Takemoto, *Chem. Lett.* **1987**, 605–608; b) K. Miki, A. Masui, N. Kasai. M. Miyata, M. Shibakami, K. Takemoto, *J. Am. Chem. Soc.* **1988**, *110*, 6594–6596; c) K. Miki, N. Kasai, M. Shibakami, K. Takemoto, M. Miyata, *J. Chem. Soc. Chem. Commun.* **1991**, 1757–1759; d) K. Nakano, K. Sada, M. Miyata, *Chem. Lett.* **1994**, 137–140; e) K. Nakano, K. Sada, M. Miyata, *J. Chem. Soc. Chem. Commun.* **1995**, 953–954; f) K. Nakano, K. Sada, M. Miyata, *Mol. Cryst. Liq. Cryst.* **1996**, *276*, 129–132.

[20] a) M. Shibakami, A. Sekiya, *J. Chem. Soc. Chem. Commun.* **1994**, 429 – 430; b) M. Shibakami, A. Sekiya, *J. Inclusion Phenom.* **1994**, *18*, 397 – 412; c) M. Shibakami, M. Tamura, A. Sekiya, *J. Inclusion Phenom.* **1995**, *22*, 155 – 168; d) M. Shibakami, M. Tamura, A. Sekiya, *J. Inclusion Phenom.* **1995**, *22*, 299 – 311; e) M. Shibakami, M. Tamura, A. Sekiya, *J. Am. Chem. Soc.* **1995**, *117*, 4499 – 4505.

[21] a) M. R. Caira, L. R. Nassimbeni, J. L. Scott, *J. Chem. Soc. Chem. Commun.* **1993**, 612 – 613; b) M. R. Caira, L. R. Nassimbeni, J. L. Scott, *J. Chem. Soc. Perkin Trans. 2* **1994**, 623 – 628; c) M. R. Caira, L. R. Nassimbeni, J. L. Scott, *J. Chem. Soc. Perkin Trans. 2* **1994**, 1403 – 1405; d) J. L. Scott, *J. Chem. Soc. Perkin Trans. 2* **1995**, 495 – 502; e) J. L. Scott, *Supramol. Chem.* **1996**, *7*, 201 – 207.

[22] a) M. Gdaniec, T. Polonski, *J. Am. Chem. Soc.* **1998**, *120*, 7353 – 7354; b) M. Gdaniec, M. Milewska, T. Polonski, *Angew. Chem.* **1999**, *111*, 405 – 408; *Angew. Chem. Int. Ed.* **1999**, *38*, 392 – 395.

[23] *Cerius*^{2}, Molecular Simulation Software, Molecular Simulation Inc..

[24] The mean values of the host cavities in the *α-gauche* and *β-trans* lattice are 247 ± 11 Å^3 and 307 ± 10 Å^3, respectively, when the cavity volume was calculated with 1.0 Å radius probe.

[25] a) M. H. Klapper, *Biochim. Biophys. Acta* **1971**, *229*, 557 – 566; b) F. M. Richards, *Ann. Rev. Biophys. Bioeng.* **1977**, *6*, 151 – 176; c) F. M. Richards, *J. Mol. Biol.* **1974**, *82*, 1 – 14.

[26] TEXSAN, X-ray Structure Analysis Package; Molecular Structure Corporation, The Woodlands, TX, **1985**.

[27] H. Nakano, *Molecular Graphics*, Science House, Tokyo, **1987**.

[28] R. Voorintholt, M. T. Kosters, G. Vegter, G. Vriend, W. G. J. Hol, *J. Mol. Graphics* **1989**, *7*, 243 – 245.

Received: June 20, 2000 [F2555]

0947-6539/01/0701-0220 $ 17.50+.50/0